

Accumulation boundaries: codimension-two accumulation of accumulations in phase diagrams of semiconductor lasers, electric circuits, atmospheric and chemical oscillators

BY CRISTIAN BONATTO AND JASON ALFREDO CARLSON GALLAS*

*Instituto de Física, Universidade Federal do Rio Grande do Sul,
91501-970 Porto Alegre, Brazil*

We report high-resolution phase diagrams for several familiar dynamical systems described by sets of ordinary differential equations: semiconductor lasers; electric circuits; Lorenz-84 low-order atmospheric circulation model; and Rössler and chemical oscillators. All these systems contain chaotic phases with highly complicated and interesting *accumulation boundaries*, curves where networks of stable islands of regular oscillations with ever-increasing periodicities accumulate systematically. The experimental exploration of such codimension-two boundaries characterized by the presence of infinite *accumulation of accumulations* is feasible with existing technology for some of these systems.

Keywords: nonlinear optics; phase diagrams; parameter space; chaos in lasers; shrimps in lasers; electric circuits

1. Introduction

The aim of this work is to report a number of very high-resolution phase diagrams for a few familiar dynamical systems with the aim of stimulating experimental work to corroborate several new features discovered in them. A key novelty reported here is that chaotic phases of dynamical systems modelled by coupled sets of nonlinear ordinary differential equations contain certain *parameter networks* with characteristic *accumulation boundaries* in phase diagrams, and many levels of self-similar behaviours, as might be recognized from figures 1 and 2. Here we illustrate for a few systems the relative abundance, shape and structuring of such networks of accumulations seen to exist abundantly in phase diagrams.

Figures 1 and 2 are high-resolution phase diagrams obtained by computing the spectra of Lyapunov exponents for the standard rate equation model of the laser, defined by equations (2.1*a*) and (2.1*b*). The boundaries of the chaotic laser phases contain certain segments (as the black–yellow transition boundary indicated by the letter A in figure 2*a*) along which wide networks of islands of regular oscillations with increasingly higher periodicities accumulate systematically. Such accumulation boundaries, limiting curves defined by the infinite network of

* Author for correspondence (jgallas@if.ufrgs.br).

One contribution of 14 to a Theme Issue ‘Experimental chaos II’.

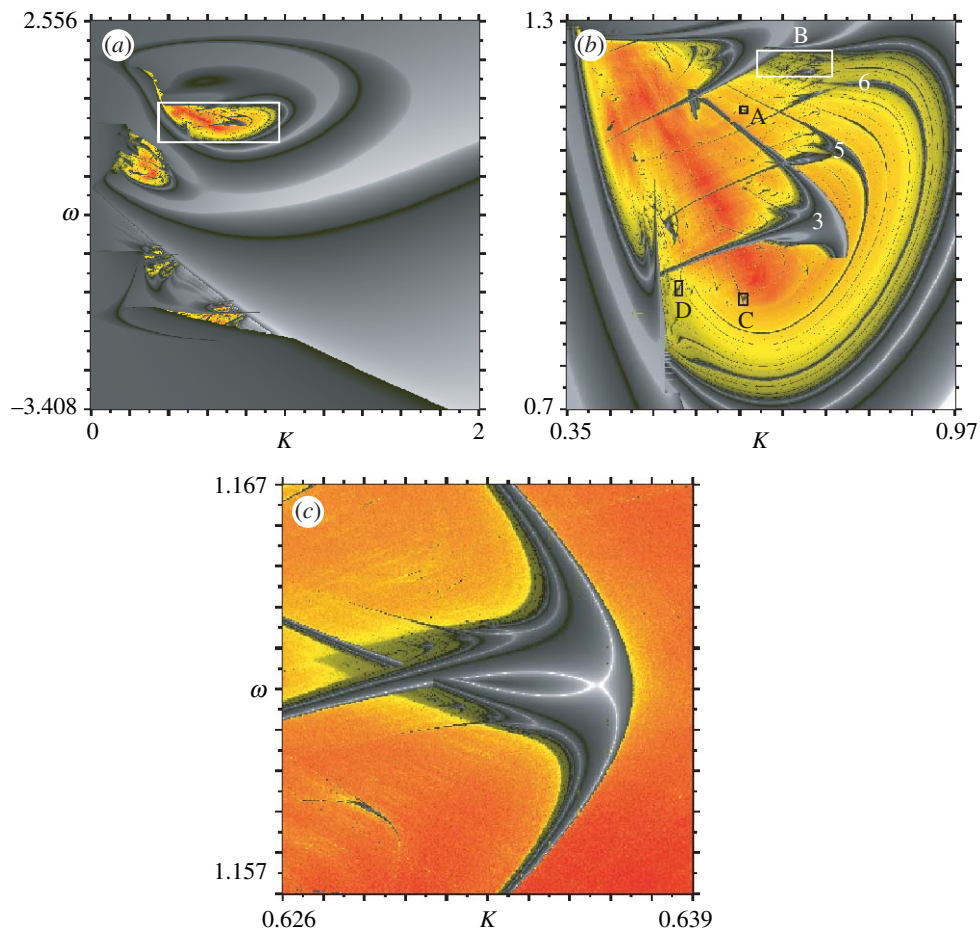


Figure 1. Phase diagrams discriminating chaos (in colours) from regularity (grey shadings). (a) Global view of parameter space. (b) Magnification of the box seen in (a), for positive detunings: numbers indicate quantity of peaks inside a period of the laser intensity. A, B, C and D mark small boxes shown magnified in the next figures. (c) Magnification of box A in (b), showing a structure similar to those recently discovered in CO₂ lasers (Bonatto *et al.* 2005).

islands, do not seem to have been observed before, not even for the computationally much less-demanding discrete-time dynamical systems where they must certainly exist. These are truly codimension-two phenomena.

Since clean and extended domains of chaos are important for a number of applications, e.g. for secure communications (Kane & Shore 2005; Ohtsubo 2005), it seems natural to inquire about what exactly is embedded in the seas of chaos abundant in dynamical systems. This is the leitmotiv here, for different types of dynamical systems. First, we discuss a semiconductor laser with injection.

2. Case study: semiconductor laser with injection

It is well known that semiconductor lasers present a rich nonlinear phenomenology when subjected to optical injection, optical feedback or modulations (Dorn *et al.* 2003; Kane & Shore 2005; Ohtsubo 2005). In particular, optically injected

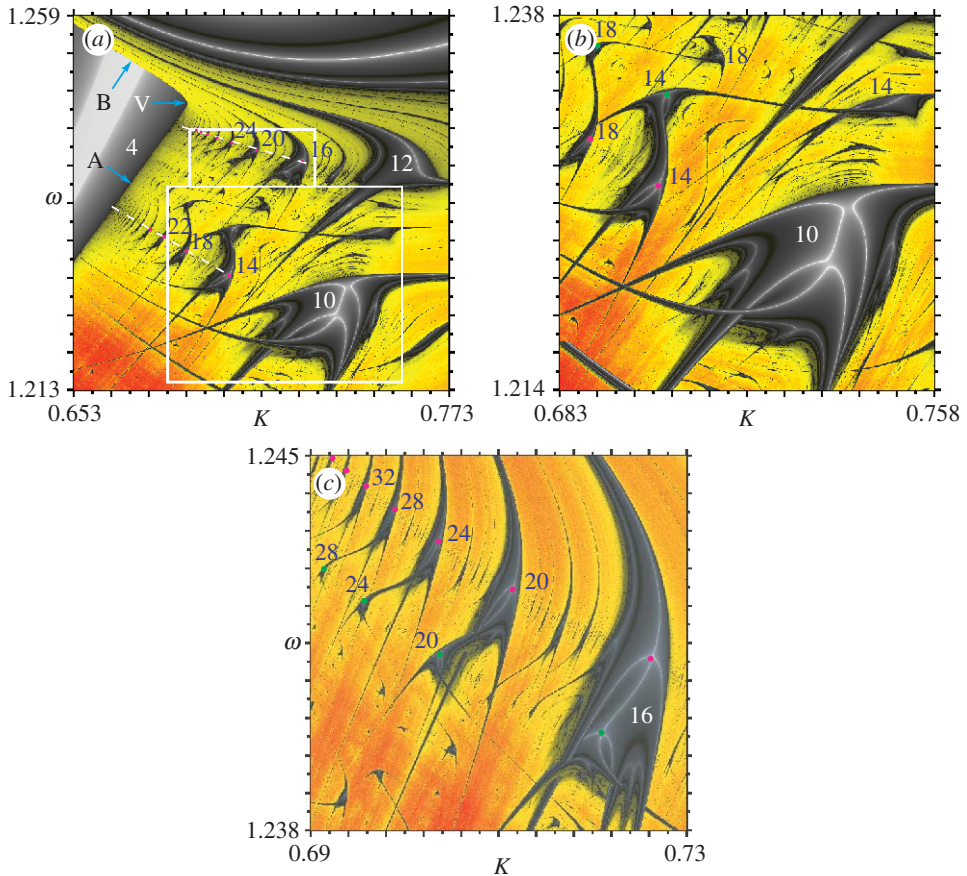


Figure 2. The several types of accumulations of periodic laser oscillations (dark islands) embedded in yellow–red sea of chaos. Numbers refer to the number of peaks of the laser amplitude. (a) The larger central bodies accumulate towards line A while stability ‘legs’ accumulate parallel to line B. Curves A and B meet at vertex V. Bifurcation diagrams along dotted lines, shown in figure 4, display typical period-adding cascades which accumulate towards the four-peak domain indicated in the upper-left corner. (b) Genesis and separation of two distinct $10 \rightarrow 14 \rightarrow 18 \rightarrow \dots$ period-adding cascades. (c) Similar genesis and separation as in (b) but now for two distinct $(12) \rightarrow 16 \rightarrow 20 \rightarrow 24 \rightarrow \dots$ cascades.

semiconductor lasers have attracted much attention in recent years, experimentally as well as from a theoretical and numerical point of view, as summarized in a recent survey by [Wieczorek *et al.* \(2005\)](#).

As mentioned, theoretical and numerical works based on a rate equation model have revealed a complex structure of bifurcations in parameter space as a function of the injected intensity and the frequency detuning. [Simpson *et al.* \(1997\)](#) located experimentally a number of bifurcations while [Wieczorek *et al.* \(2002\)](#) compared measurements with numerical computations, obtaining a very good overall agreement between theory and experiments.

Theoretical calculations ([Gao *et al.* 1999](#)) and numerical simulations ([Hwang & Liu 2000](#)) predicted intricate laser behaviours, including stable solutions inside domains characterized by chaotic laser oscillations. Recently, [Chlouverakis & Adams \(2003\)](#) and [Fordell & Lindberg \(2004\)](#) reported a series of

stability diagrams obtained by direct numerical integration of the rate equations for an optically injected semiconductor laser, where it is possible to identify various stability islands embedded in a sea of chaos. However, not much is presently known about the shape, abundance and structuring of such stability islands.

The single-mode semiconductor laser subjected to monochromatic optical injection is well described by rescaled rate equations for the complex laser field $E = E_x + iE_y$ and population inversion n

$$\dot{E} = K + \left(\frac{1}{2}(1 + i\alpha)n - i\omega\right)E \quad \text{and} \quad (2.1a)$$

$$\dot{n} = -2\Gamma n - (1 + 2Bn)(|E|^2 - 1). \quad (2.1b)$$

Here, the control parameters are the intensity K of the injected field and ω , the detuning frequency. The remaining parameters are defined as usual: $B=0.0295$, $\Gamma=0.0973$ and $\alpha=2.6$ (Wieczorek *et al.* 2002).

Figure 1 shows phase diagrams obtained by integrating the above equations with a standard four-order Runge–Kutta scheme with a fixed step $h=0.01$. The Lyapunov spectra are computed using *farming* (Zeni & Gallas 1995). Parameter grid points were colour codified according to the magnitude of the largest non-zero exponent: regions of negative exponents (periodic solutions) are coloured grey (black indicates zero, white the most negative values), while positive exponents (chaotic laser oscillations) are indicated in a yellow–red scale. Red indicates regions of stronger chaos, characterized by more positive exponents. The colour scale of individual phase diagrams was renormalized to cover the interval of exponents contained in the diagram.

Several bifurcation boundaries for orbits of low period as well as saddle-node and Hopf bifurcations have been recently reported theoretically and experimentally by Wieczorek *et al.* (2002) and Al-Hosiny *et al.* (2007). However, in addition to such bifurcation boundaries, our phase diagrams show details and regularities not observed before, now including all regions of periodic oscillations and the regions of chaos. Our phase diagrams show the inner details and structuring of stability domains, the regions where a recurring self-similar organization occurs and where it fails to exist.

In a pioneering work, Eriksson & Lindberg (2001, 2002) measured experimentally the location and magnitude of islands characterized by regular oscillations existing inside chaotic phases of semiconductor lasers. First, they identified a period-3 island by tuning the injection intensity for three fixed values of the frequency detuning. Then, by repeating measurements for finer detuning intervals, they cleverly managed to characterize a few islands of low period. Figure 1*b* corroborates their low-periodic islands and shows a myriad of additional islands of ever-increasing periods as discussed below. The figure also displays several novel features, in particular the existence of self-similarities of various kinds. Figure 1*c* displays an island with a familiar shrimp-shaped complex structure recorded when varying two parameters simultaneously (codimension-two phenomenon). Although well known in *discrete*-time dynamical systems (Gallas 1993, 1994, 1995), this peculiar shrimp-shaped structure was observed only quite recently in a *continuous*-time system, namely in CO₂ lasers (Bonatto *et al.* 2005).

The above-mentioned striking and unexpected accumulation networks may be easily recognized from the phase diagrams of figure 2, which present successively magnified views of box B in figure 1*b*. Embedded in the chaotic region, there are regular and abundant networks of stable islands of periodic laser oscillations with unbounded periodicities. As figure 2*a* shows, the parameter networks living in the chaotic region bridge periodic laser oscillations of increasingly higher periodicities and which converge systematically towards well-defined and characteristic accumulation boundaries. As indicated schematically by the numbers in figure 2*a*, when moving along the dark central bodies of the islands one observes series of *period-adding cascades* of bifurcations, a characteristic signature of the experimentally elusive and rather challenging homoclinic route to chaos (Braun *et al.* 1992).

That stability organizes along specific *directions* in parameter space is a well-known fact for discrete-time dynamical systems (Gallas 1993, 1994, 1995). But that the same is true for continuous-time dynamical system is now made obvious by figure 2. But a rather unexpected novel feature clearly discernible in figure 2*b* is the surprising way in which individual period-adding bifurcation cascades are born. As seen, the pair of osculating white spines living inside the large dark island of period-10 oscillations *splits* as the period increases, leading to separate cascades that quickly give the impression of being uncorrelated owing to the strong compression experienced by the islands as the period increases more and more without bound. The white spine indicate loci of the most negative Lyapunov exponents and are loosely ‘equivalent’ to the familiar superstable orbits in discrete-time dynamical systems. The splitting process involves several specific metric properties, for instance the parameter separation of the islands accumulates to specific values while their volume decreases regularly with characteristic exponents (Bonatto & Gallas 2007).

As another remarkable result found in phase diagrams of differential equations, figure 3 illustrates two islands of regular oscillations with the same exquisite shape and structuring found very recently in a rather different scenario: in a discrete-time dynamical system with no critical points, i.e. in a dynamical system not obeying the Cauchy–Riemann conditions (Endler & Gallas 2006). Such striking shapes and structures exist abundantly in a continuous-time system, in the lower portion of figure 1*b*. Thus, semiconductor lasers open the way to investigate experimentally novel and sophisticated mathematical behaviours resulting from dynamics not ruled by critical points, so far believed to be the major players in the dynamics of complex functions (Endler & Gallas 2006).

How can one detect experimentally the existence of accumulation networks embedded in chaos? One simple answer is provided by the bifurcation diagrams in figure 4, showing the unfolding of the period-adding cascades, as recorded independently for each dynamical variable, E_x , E_y and n , and the laser intensity $I \equiv E_x^2 + E_y^2$. These diagrams clearly show the period-adding cascades, with the clear alternation of windows of chaos and periodic oscillations. In these diagrams, the numbers labelling periodic windows refer to the number of peaks present in one period of the respective variable. However, different variables display *different* number of peaks. Since the number of peaks is usually taken to label the ‘period’ of oscillation, one sees that such labels *depend on the variable used to count the peaks*. In particular, the numerical labels in figure 2 would be different had we used, say, the population inversion n instead of the laser amplitude I to count peaks. Clearly, the fact that local maxima of E_x and E_y occur here at distinct instants introduces a

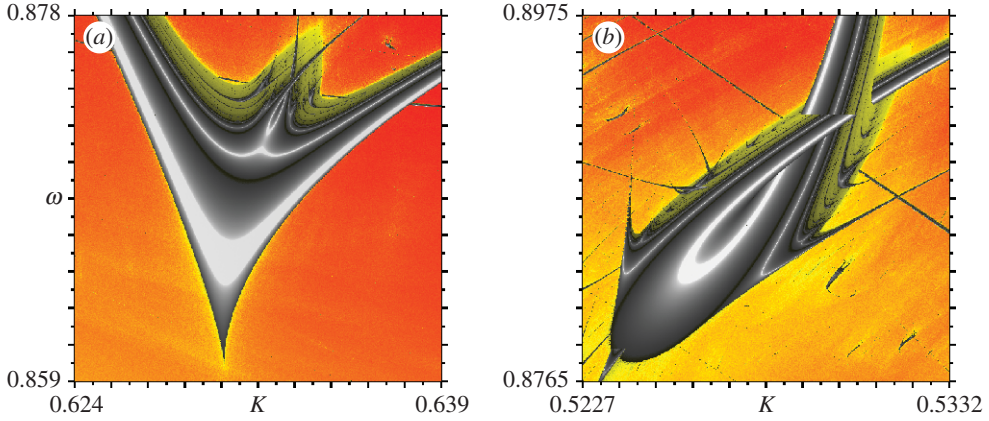


Figure 3. Magnification of boxes B and C in figure 1b, illustrating differential equations, shapes and structures identical with those found recently in maps and in a very different scenario: in systems having no critical points. (a) Cuspidal island and (b) non-cuspidal island.

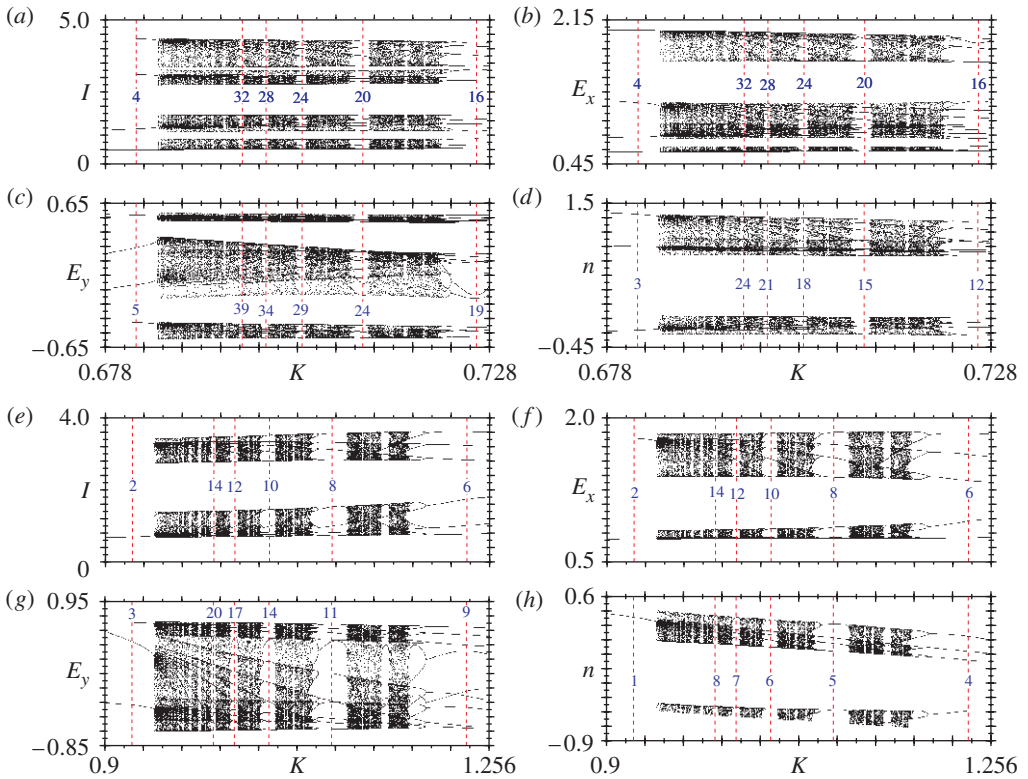


Figure 4. Periodic windows are easier to measure for higher values of α . (a) Bifurcation diagrams obtained for $\alpha=2.6$ while moving along the lower (12) \rightarrow 16 \rightarrow 20 \rightarrow 24 \rightarrow ... cascade shown in figure 2a,c. (b) Bifurcation diagrams for $\alpha=6.0$ along the cascade shown in figure 5a. Note that the period-9 window in E_y does not belong to the adding cascade. The numbering of the windows in each diagram depends of the number of peaks of the quantity considered.

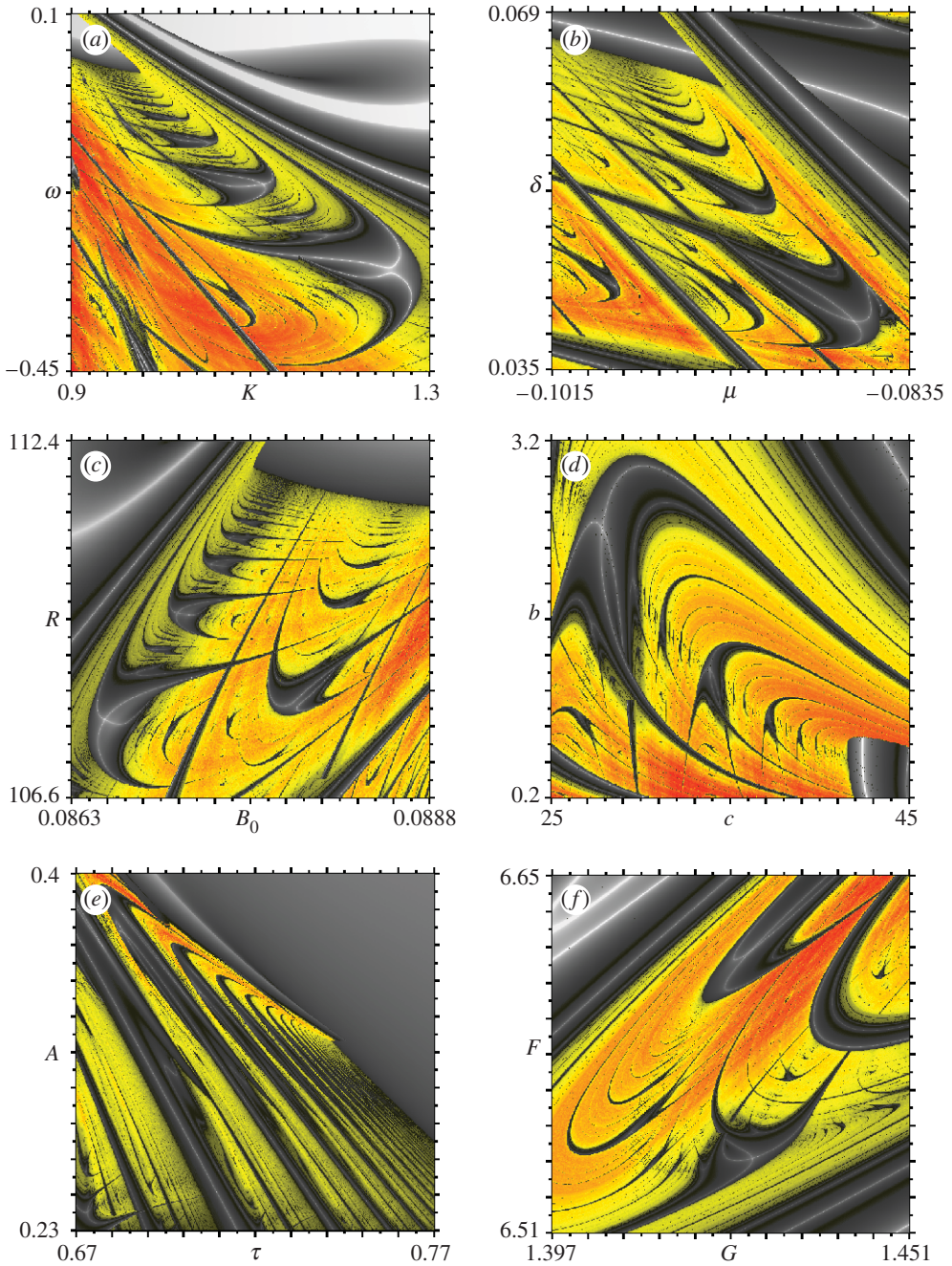


Figure 5. Accumulation of accumulations in phase diagrams of six different continuous-time physical systems. (a) Optically injected semiconductor laser for $\alpha=6.0$, (b) CO₂ laser with feedback (Pisarchik *et al.* 2001), (c) autonomous electronic circuit (Freire *et al.* 1984), (d) Rössler system with $a=0.2$ (Rössler 1976), (e) Non-autonomous chemical model (Vance & Ross 1989) and (f) Lorenz-84 low-order atmospheric circulation model (Bonatto *et al.* submitted; Freire *et al.* submitted). The meaning of the parameters is defined below and in the papers quoted.

rather complicated Lissajous-like phase dependence responsible for the number of local maxima of I , which is very hard to predict. We observe that even in situations where direct measurement of the laser intensity might be difficult, a feasible alternative is to measure the spectrum of frequencies.

3. Lasers, electric circuits, Rössler and chemical oscillators

Are the regularities and accumulations described above for the optically injected semiconductor laser also found in other dynamical systems ruled by sets of nonlinear ordinary differential equations? The answer is yes. To corroborate our affirmative answer, [figure 5](#) presents phase diagrams for several rather distinct dynamical systems without entering into discussions, due to space limitations. We simply give equations and parameters used to generate these phase diagrams. For additional details concerning the equations, we refer to the original references.

Interesting homoclinic phenomena are well known to exist in the following model of a CO₂ laser with feedback, as described by [Pisarchik *et al.* \(2001\)](#):

$$\dot{x}_1 = k_0 x_1 (x_2 - 1 - k_1 \sin^2 x_6), \quad (3.1a)$$

$$\dot{x}_2 = -\Gamma_1 x_2 - 2k_0 x_1 x_2 + \gamma x_3 + x_4 + P_0, \quad (3.1b)$$

$$\dot{x}_3 = -\Gamma_1 x_3 + x_5 + \gamma x_2 + P_0, \quad (3.1c)$$

$$\dot{x}_4 = -\Gamma_2 x_4 + \gamma x_5 + z x_2 + z P_0, \quad (3.1d)$$

$$\dot{x}_5 = -\Gamma_2 x_5 + z x_3 + \gamma x_4 + z P_0 \quad \text{and} \quad (3.1e)$$

$$\dot{x}_6 = -\beta x_6 + \beta B_0 - \beta f(x_1), \quad (3.1f)$$

where $f(x_1) = R x_1 / (1 + \alpha x_1)$ is the *feedback* function. We used the same parameters considered by [Pisarchik *et al.* \(2001\)](#), namely $\Gamma_1 = 10.0643$, $\Gamma_2 = 1.0643$, $\alpha = 32.8767$, $\beta = 0.4286$, $k_0 = 28.5714$, $k_1 = 4.5556$ and $P_0 = 0.016$.

The third model considered here is a modification of the original Van der Pol circuit, proposed originally by [Shinriki *et al.* \(1981\)](#). It consists of an autonomous electronic circuit involving a resonant circuit and two nonlinear conductances, one positive and the other negative. Motivated by the interesting circuit of [Shinriki *et al.* \(1981\)](#), [Freire *et al.* \(1984\)](#) have shown shortly after that such circuit displays a rich variety of dynamical behaviours. The circuit is described by the following set of time-independent equations:

$$C_0 \dot{x} = (a_1 - G_1)x - a_3 x^3 + b_1(y - x) + b_3(y - x)^3, \quad (3.2a)$$

$$C \dot{y} = -G_2 y - z - b_1(y - x) - b_3(y - x)^3 \quad \text{and} \quad (3.2b)$$

$$L \dot{z} = y, \quad (3.2c)$$

where the bifurcation parameters shown in the figure are $\mu = G_1 + b_1 - a_1$ and $\delta = G_2 + b_1$, and we consider the same parameters used by [Freire *et al.* \(1984\)](#): $C_0 = 4.7$ nF, $C = 100$ nF, $L = 110$ mH, $a_1/\omega C = 0.1$, $a_3/\omega C = 6 \times 10^{-4}$, $b_1/\omega C = 0.016$ and $b_3/\omega C = 0.05$.

The fourth model considered is the 40-year-old equations introduced by Rössler (1976)

$$\dot{x} = -y - z, \quad (3.3a)$$

$$\dot{y} = x + ay \quad \text{and} \quad (3.3b)$$

$$\dot{z} = b + zx - zc. \quad (3.3c)$$

In our simulations, we fixed $a \equiv 0.2$.

The next model considered represents a time-periodically forced chemical oscillator studied by Vance & Ross (1989) and Hou & Xin (1999) and described by the equations

$$\dot{x} = 1 - x - xDE(y) + p(t)(1 - x) \quad \text{and} \quad (3.4a)$$

$$(1 + \epsilon)\dot{y} = -\beta y + BDE(y) - p(t)(y - \gamma), \quad (3.4b)$$

where

$$E(y) = \exp\left(\frac{y}{1 + \eta y}\right) \quad \text{and} \quad p(t) = A \sin\left(\frac{2\pi t}{\tau T_0}\right). \quad (3.5)$$

Here, following Vance & Ross (1989) and Hou & Xin (1999), we also considered their point $P_2 = (j, T_c) = (0.8, 292)$ where the system exhibits self-oscillations with period $T_0 = 4.1627372$ in absence of forcing. The other parameters are the following: $\epsilon = 0.65$; $T^* = 885.843j + 11.02T_c / (2.7j + 11.02)$; $\eta = T^* / 8827$; $D = 8.2365 \times 10^{10} e^{-1/\eta/j}$; $B = 271.46 / (\eta T^*)$; and $\beta = 1 + 4.08/j$. As indicated in figure 5, the bifurcation parameters are A and τ . Our figures contain a wealth of new details, including cascades of accumulations.

Finally, we also considered Lorenz-84 low-order atmospheric circulation model (Lorenz 1984), a model containing rich accumulations and homoclinic phenomena with meteorological implications (Freire *et al.* 2007):

$$\dot{x} = -y^2 - z^2 - ax + aF, \quad (3.6a)$$

$$\dot{y} = xy - y - bxz + G \quad \text{and} \quad (3.6b)$$

$$\dot{z} = bxy + xz - z. \quad (3.6c)$$

As usual, we also considered the dynamics when fixing $a = 0.25$ and $b = 4$.

Each of these systems has a number of additional interesting aspects involving homoclinic phenomena and their consequences inside chaotic regions in parameter space. These are discussed in detail elsewhere. Here, the purpose is simply to emphasize that the accumulations and the accumulation of accumulations lying in ‘simple’ curves are generic phenomena found profusely in nonlinear systems of ordinary differential equations. Note that while differential equations have been around for quite a while, thus far no phase diagrams reporting the hierarchical structuring of the chaotic phases seem to exist in the literature.

4. Final remarks

We have shown that chaotic regions in phase diagrams of a number of dynamical systems ruled by sets of nonlinear ordinary differential equations contain very peculiar hierarchies of parameter networks ending in distinctive accumulation boundaries characterized by an infinite amount of accumulation of accumulations, with very rich and interesting structuring. The systems discussed here were semiconductor lasers with optical injection, CO₂ lasers with feedback, autonomous electric circuits, the Rössler oscillator, Lorenz-84 low-order atmospheric circulation model and a chemical model. Since accumulation of accumulations was found in all these distinct physical models, we believe them to be the generic features of dynamical systems of codimension-two and higher.

The network of regularity islands found to exist embedded in chaotic phases may compromise applications depending on ‘smooth and clean domains of chaos’ such as secure communications. The parameter networks reported here pose an interesting question that remains to be investigated: in sharp contrast with discrete dynamical systems, where periods vary in discrete units, an appealing new possibility afforded by lasers is to study how periodicities defined by continuous real numbers evolve in phase diagrams when parameters are tuned. Additionally, another enticing question is whether or not it is possible to infer the presence of homoclinic orbits in phase space from regularities computed/measured solely in the parameter space. Are there clear parameter-space signatures of homoclinic orbits? Is it possible to recognize the location of parameter loci characterizing simple and multiple (degenerate) homoclinic phenomena in phase diagrams? These questions are the subject of a separate work.

The few points addressed here so far do not exhaust the richness of phenomena found in phase diagrams of continuous-time dynamical systems. As a last example, [figure 6](#) illustrates families of isoperiodic parameter circles found in a CO₂ laser with modulated losses. The equations and parameters used to produce [figure 6](#) are those of [Bonatto *et al.* \(2005\)](#), with a single exception: here we use $z_0=0.18$. When changing parameters inside such circles, the shape and the length of the periodic signals change but the number of peaks inside the circle period remains the same. An obvious question is that concerning the unfolding of these circles when other model parameters are varied, i.e. when considered as higher codimensional events. We have also seen a profusion of infinite hierarchies of nested spirals. This needs to be investigated.

As a last remark, it is perhaps interesting to emphasize that while accumulating regions of periodic orbits in optically driven lasers have been recently reported by [Krauskopf & Wicczorek \(2002\)](#), the phenomenon they describe is rather different from those reported here. For, as summarized in the comparisons presented in [figure 7](#), they consider domains of periodic orbits, not regions of chaos as we do. Their accumulations involve saddle-node–Hopf bifurcations while ours do not. They investigate accumulations towards a fixed point while ours involve more complex objects. In addition, note that while [Krauskopf & Wicczorek \(2002\)](#) argue period-adding routes to chaos not to be present in semiconductor lasers, we find such routes to occur in profusion. A detailed discussion of these matters will be presented elsewhere.

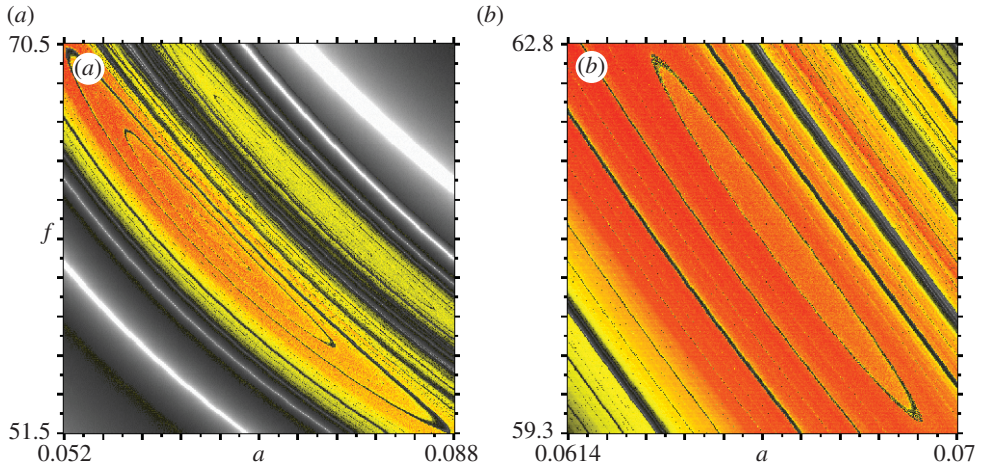


Figure 6. Families of isoperiodic parameter circles found for a CO₂ laser with modulated losses. When changing parameters inside one of these circles, the shape and the length of the periodic signals change but the number of peaks inside a period remains the same. (a) Global view and (b) magnified view of the central circle. Frequencies f are in kHz (Bonatto *et al.* 2005).

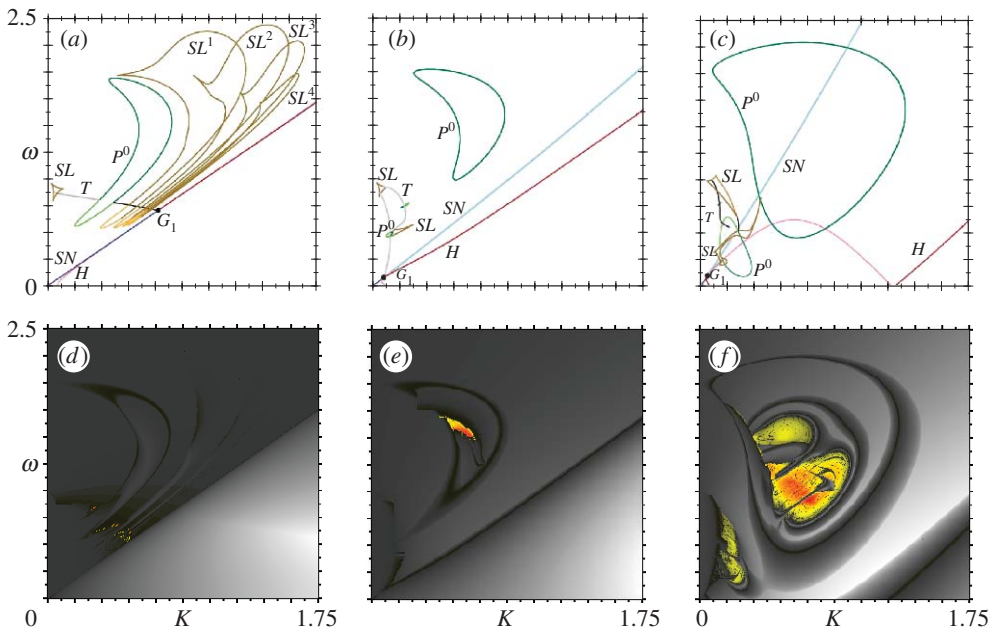


Figure 7. (a–c) Low-period boundary curves in the vicinity of a simultaneous saddle-node and Hopf bifurcations, for $\alpha=0.0, 0.5$ and 2.0 , according to Krauskopf & Wiecek (2002). (d–f) Phase diagrams including periodic and chaotic phases. The accumulation boundaries described here in figures 2 and 5, containing an infinite number of accumulation of accumulations, are not observed near this saddle-node–Hopf point of the laser.

The authors are indebted to Prof. F.T. Arecchi for drawing their attention to the Shilnikov phenomena in the CO₂ laser model reported by Pisarchik *et al.* (2001). They also thank the Conselho Nacional de Desenvolvimento Científico e Tecnológico, Brazil, for a doctoral fellowship (C.B.) and a senior research fellowship (J.A.C.G.). This work was supported by the Air Force Office of Scientific Research, through contract FA9550-07-1-0102.

References

- Al-Hosiny, N., Henning, I. D. & Adams, M. J. 2007 Tailoring enhanced chaos in optically injected semiconductor lasers. *Opt. Commun.* **269**, 166–173. (doi:10.1016/j.optcom.2006.07.066)
- Bonatto, C. & Gallas, J. A. C. 2007 Accumulations horizons and period adding cascades in optically injected semiconductor lasers. *Phys. Rev. E* **75**, 055204(R). (doi:10.1103/PhysRevE.75.055204)
- Bonatto, C., Garreau, J. C. & Gallas, J. A. C. 2005 Self-similarities in the frequency–amplitude space of a loss-modulated CO₂ laser. *Phys. Rev. Lett.* **95**, 143905. (doi:10.1103/PhysRevLett.95.143905)
- Bonatto, C., Freire, J. G. & Gallas, J. A. C. Submitted. Accumulation of bifurcations and multistability in the Lorenz-84 low-order atmospheric circulation model.
- Braun, T., Lisboa, J. A. & Gallas, J. A. C. 1992 Evidence of homoclinic behavior in the plasma of a glow discharge. *Phys. Rev. Lett.* **68**, 2770–2773. (doi:10.1103/PhysRevLett.68.2770)
- Chlouverakis, K. E. & Adams, M. J. 2003 Stability maps of injection-locked laser diodes using the largest Lyapunov exponent. *Opt. Commun.* **216**, 405–412. (doi:10.1016/S0030-4018(02)02357-X)
- Dorn, R., Quabis, S. & Leuchs, G. 2003 Sharper focus for a radially polarized light beam. *Phys. Rev. Lett.* **91**, 233901. [See also *Phys. Rev. Focus* **12**, story 19. van de Nes, A. S. *et al.* 2006 *Rep. Prog. Phys.* **69**, 2323]. (doi:10.1103/PhysRevLett.91.233901)
- Endler, A. & Gallas, J. A. C. 2006 Mandelbrot-like sets in dynamical systems with no critical points. *C.R. Acad. Sci. Paris, Series I* **342**, 681–684.
- Eriksson, S. & Lindberg, A. M. 2001 Periodic oscillation within the chaotic region in a semiconductor laser subjected to external optical injection. *Opt. Lett.* **26**, 142–144.
- Eriksson, S. & Lindberg, A. M. 2002 Observations on the dynamics of semiconductor lasers subjected to external optical injection. *J. Opt. B: Quantum Semiclassical Opt.* **4**, 149–154. (doi:10.1088/1464-4266/4/2/311)
- Fordell, T. & Lindberg, A. M. 2004 Numerical stability maps of an optically injected semiconductor laser. *Opt. Commun.* **242**, 613–622. (doi:10.1016/j.optcom.2004.09.009)
- Freire, E., Franquelo, L. G. & Aracil, J. 1984 Periodicity and chaos in an autonomous electronic system. *IEEE Trans. Circ. Syst.* **31**, 237–247. (doi:10.1109/TCS.1984.1085496)
- Freire, J. G., Bonatto, C., daCamara, C. & Gallas, J. A. C. Submitted. Intransitivity diagrams for the Lorenz-84 low-order atmospheric circulation model.
- Gallas, J. A. C. 1993 Structure of the parameter space of the Hénon map. *Phys. Rev. Lett.* **70**, 2714–2717. (doi:10.1103/PhysRevLett.70.2714)
- Gallas, J. A. C. 1994 Dissecting shrimps: results for some one-dimensional systems. *Physica A* **202**, 196–223. (doi:10.1016/0378-4371(94)90174-0)
- Gallas, J. A. C. 1995 Structure of the parameter space of a ring cavity. *Appl. Phys. B* **60**, S203–S213. (doi:10.1007/BF01135875)
- Gao, J. B., Hwang, S. K. & Liu, J. M. 1999 Effects of intrinsic spontaneous-emission noise on the nonlinear dynamics of an optically injected semiconductor laser. *Phys. Rev. A* **59**, 1582–1585. (doi:10.1103/PhysRevA.59.1582)
- Hou, Z. & Xin, H. 1999 Stochastic resonance in the presence or absence of external signal in the continuous stirred tank reactor system. *J. Chem. Phys.* **111**, 721–723. (doi:10.1063/1.479350)
- Hwang, S. K. & Liu, J. M. 2000 Dynamical characteristics of an optically injected semiconductor laser. *Opt. Commun.* **183**, 195–205. (doi:10.1016/S0030-4018(00)00865-8)
- Kane, D. M. & Shore, K. A. 2005 *Unlocking dynamical diversity: optical feedback effects on semiconductor lasers*. New York, NY: Wiley.

- Krauskopf, B. & Wieczorek, S. 2002 Accumulating regions of winding periodic orbits in optically driven lasers. *Physica D* **173**, 97–113. (doi:10.1016/S0167-2789(02)00650-4)
- Lorenz, E. N. 1984 Irregularity: a fundamental property of the atmosphere. *Tellus A* **36**, 98–110.
- Ohtsubo, J. 2005 *Semiconductor lasers: stability instability and chaos*. New York, NY: Springer.
- Pisarchik, A. N., Meucci, R. & Arcelli, F. T. 2001 Theoretical and experimental study of discrete behavior of Shilnikov chaos in a CO₂ laser. *Eur. Phys. J. D* **13**, 385–391. (doi:10.1007/s100530170257)
- Rössler, O. E. 1976 Equation for continuous chaos. *Phys. Lett. A* **57**, 397–398. (doi:10.1016/0375-9601(76)90101-8)
- Shinriki, M., Yamamoto, M. & Mori, S. 1981 Multimode oscillations in a modified Van der Pol oscillator containing a positive nonlinear conductance. *Proc. IEEE* **69**, 394–395.
- Simpson, T. B., Liu, J. M., Huang, K. F. & Tai, K. 1997 Nonlinear dynamics induced by external optical injection in semiconductor lasers. *Quantum Semiclassical Opt.* **9**, 765–784. (doi:10.1088/1355-5111/9/5/009)
- Vance, W. & Ross, J. 1989 A detailed study of a forced chemical oscillator: Arnold tongues and bifurcation sets. *J. Chem. Phys.* **91**, 7654–7670. (doi:10.1063/1.457235)
- Wieczorek, S., Simpson, T. B., Krauskopf, B. & Lenstra, D. 2002 Global quantitative predictions of complex laser dynamics. *Phys. Rev. E* **65**, 45207R. (doi:10.1103/PhysRevE.65.045207)
- Wieczorek, S., Krauskopf, B., Simpson, T. B. & Lenstra, D. 2005 The dynamical complexity of optically injected semiconductor lasers. *Phys. Rep.* **416**, 1–128. (doi:10.1016/j.physrep.2005.06.003)
- Zeni, A. R. & Gallas, J. A. C. 1995 Lyapunov exponents for a Duffing oscillator. *Physica D* **89**, 71–83. (doi:10.1016/0167-2789(95)00215-4)